Rayleigh-Bénard Convection

Introduction

The Rayleigh-Bénard (henceforth referred to as RB) system has been studied by researchers for a complete century by now and is still a topic of interest to them. It would be interesting to find out why? The R-B problem is relevant to applications ranging from astrophysics (where e.g., the validity of star models depends to a large degree on the validity of energy transport in the outer regions of stellar atmospheres), geophysics (where e.g., the current theories of continental drift depend on possible convective motion in the earth's mantle caused by internal heat generation due to radioactive decay), and atmospheric sciences (where e.g., theories and prediction of current weather phenomena as well as long-term effects like ice ages depend on the validity of theories of convective energy transport in the Earth's atmosphere). It's applications to various engineering systems, such as Solar Energy systems, material processing, energy storage, and nuclear systems are numerous.

Apart from its relevance to the various branches of engineering and physical sciences, the R-B system is being investigated for purely theoretical and fundamental reasons as well. The classical "Standard" mathematical model of this problem consists of a set of non-linear coupled partial differential equations, the solution of which is degenerate and non-unique. It, therefore, serves as a paradigm of a nonlinear system, which if investigated properly, can provide insight to the researchers studying nonlinear phenomena. It is now, generally recognized that time dependence in the R-B system offers clues to the transition from laminar to turbulent flow. It is worthwhile to note here that the transition phenomena, in general, is independent of the geometrical systems and is more a flow property, e.g., a proper choice of length scale makes the transition Reynolds Number to be identical for both flat plate and pipe flow case. In another related issue, R-B system is the most carefully studied example of nonlinear systems exhibiting self-organization or *pattern forming systems* , of special interest to researchers from Synergetic. It demonstrates essential features typical not only of various hydrodynamic instabilities but also of many non-linear pattern-forming processes differing in their nature. Formation of patterns close to spatially periodic ones can be observed in crystal growth, propagation of solidification fronts, electrohydrodynamic instabilities of nematic liquid crystals, chemical reaction-diffusion processes, auto catalytic reactions, buckling of thin plates and shells, morphogenesis of plants and animals, etc. Such patterns are also seen in cloud streets, sand ripples on flat beaches, and desert

dunes, in genealogical formations, in interacting laser beams, in the grid-scale instabilities of numerical algorithms, and in many other objects. R-B convection can be considered, as stated by Newell et. al.[1], " the grandaddy of canonical examples used to study pattern formation and behavior in spatially extended systems". It provides excellent possibilities for studying the spontaneous establishment of spatial ordering and at the same time, raises very subtle questions of the realizability of particular form and scales of flows, or the selection of those forms and scales that are in a certain sense preferred.

In this term paper, we review and highlight some of the experimental, and computational work that has been done to study the phenomena of flow transition and pattern formation and their association to stability, heat-transfer, velocity and temperature distribution.

Background

The R-B problem in its simplest form and one that was the earliest to be investigated is the so-called infinite layer case. In such a case, a layer of fluid is constrained between two infinite horizontal surfaces. The surface is heated from below, i.e., the lower surface is at a higher temperature than the upper surface. The heated from below is said to have an adverse temperature gradient because the fluid at the bottom will be lighter than the fluid at the top and this top-heavy arrangement is potentially unstable. When the temperature gradient is below a certain value, the natural tendency of the fluid to move, because of buoyancy, will be inhibited by its own viscosity and thermal diffusivity. Thus the thermal instability will manifest itself only when the adverse temperature gradient exceeds a certain critical value.

The earliest experiments to demonstrate in a definitive manner the onset of thermal instability in fluids are due to Bénard in 1900. The theoretical foundations for a correct interpretation of the phenomena are due to Rayleigh in 1916. The phenomena of thermal convection under an adverse temperature gradient is therefore known as the Rayleigh-Bénard convection in their honor. As concerns the physics of phenomena, however, combining both names in one term reflects a longstanding confusion in the comprehension of the mechanism of convection, which has not yet been completely overcome: Bénard observed a phenomena in which instability due to the temperature dependence of the surface-tension coefficient played a substantial role whereas Rayleigh studied convection caused by an instability of another type, which arises from the temperature (and density) nonuniformity of the fluid layer. Usually, the term Rayleigh-Bénard convection is attributed to convection due to Rayleigh mechanism, while the term Bénard-Marangoni convection refers to themocapillary convection.

Concepts and problem statement

Bénard, carrying out his experiments at the turn of the century, observed the establishment of a regular, steady pattern of flow cells in a thin horizontal layer of molten spermaceti with a free upper surface. These cells, which later came to be known as *Bénard cells*, were mainly hexagonal, and the patter resembled a honeycomb. Their origin is currently attributed to the temperature dependence of surface tension. Among theorists, Lord Rayleigh was the first to solve the problem of the onset of thermal convection in a plane horizontal layer of fluid heated from below.

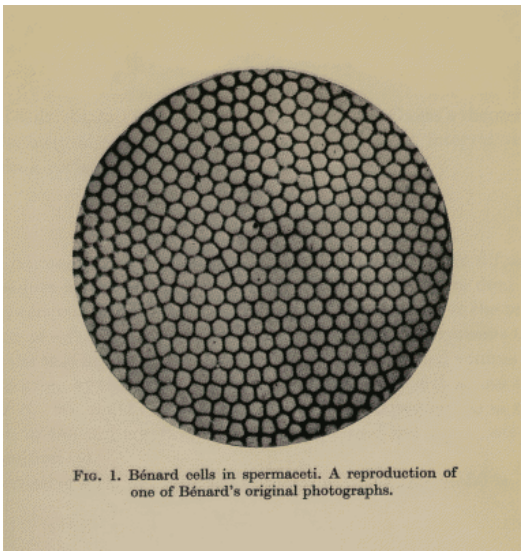

FIG. 1. Bénard cells in spermaceti. A reproduction of one of Bénard's original photographs.

Benard Cells in spermaceti. A reproduction of one of Bénard's original photograph

The statement of the R-B problem is based on the set of the hydrodynamic equations in the Oberbeck-Boussinesq approximation. With this approximation in the effect, the fluid density ρ is considered to be independent of pressure and to depend linearly on the temperature *T*:

$$\rho - \rho_0 = -\rho_0 \alpha (T - T_0)$$

where ρ_0 is the density value for some suitably chosen "mean" (or, better to say, reference) temperature T_0 . Let the volumetric coefficient of thermal expansion α be small and let the material characteristics of the fluid (kinematic viscosity ν , thermal diffusivity χ , and the coefficient α itself) vary little within the region considered (we mean the region by a horizontal layer). Then, for not-too-fast processes, the density and these characteristics can be considered to

be constant everywhere in the equations, with the only exception: The density variation must be retained in the buoyancy term, where it is multiplied by the gravity acceleration **g** (it is this term that is responsible for the phenomenon of convection). If so, heat release due to viscous dissipation is also negligible. If, in addition, the physical characteristics of the fluid are virtually constant within the volume under study, the static, barotropic temperature distribution should be a linear function of the vertical coordinate z (height): $T_s = T_1 - b\ z$ (where T_1=*const)*. Hereinafter, the subscript s means the static, or unperturbed, value of a physical variable (i.e., its value corresponding to the motionless state of the fluid). Accordingly, we call $T_s\ (z)$ the unperturbed temperature, and b the unperturbed temperature gradient. For arbitrary T, the quantity $q = T - T_s$ is termed the temperature perturbation; the deviation of the pressure from its static distribution dictated by such a linear temperature profile, the pressure perturbation p'. In this notation the Boussinesq equations have the following form:

$$\frac{\partial V}{\partial t} + (V.\nabla)V = -\frac{\nabla p'}{r_0} - \mathrm{g}a\,q + n\Delta V;$$

$$\frac{\partial q}{\partial t} + V.\nabla(T_s + q) = c\Delta q,$$

$$div\,V = 0$$

$$q = 0\ both\ boundaries,$$

$$Vz = 0, \frac{\partial Vx}{\partial z} = \frac{\partial Vy}{\partial z} = 0\ on\ both\ free\ boundaries$$

This outlined the classic R-B problem, in the original nonlinear and dimensional form. It can be nondimensionalized by taking the layer thickness h as the unit of length, the time $t_v = h^2 / c$ of vertical diffusion of heat as the unit of time, and the temperature difference ΔT between the layer boundaries as the unit of temperature. the previous equations can be written as:

$$\frac{1}{P}\left[\frac{\partial V}{\partial t}+(V.\nabla)V\right]=-\nabla w+\hat{z}\,Rq+\Delta V, \qquad ----(X)$$

$$\frac{\partial q}{\partial t}-v_z+V.\nabla q=\Delta q, \qquad ----(Y)$$

$$divV=0$$

$$Here\ R=\frac{ag\Delta Th^3}{nc},\ P=\frac{n}{c}$$

are the basic parameters characterizing the convection regime, termed the Rayleigh and the Prandtl number, respectively. *w* is the nondimensional form of the quantity p' / r_0; and z is the unit vector of the z-direction. The Rayleigh number determines the departure of the system from the equilibrium state. In accordance with the terminology commonly used in the theory of nonequilibrium systems, it is often called the control parameter.

Taking the curl of the first equation, we get in terms of vorticity ($\Omega=\nabla\ X\ V$)

$$\frac{1}{P}\left[\frac{\partial\Omega}{\partial t}-\nabla\ X\ (V\ X\ \Omega)\right]=R\nabla q\ x\hat{z}+\Delta\Omega$$

$$\Omega_z=0 \qquad on\ a\ rigid\ boundary,$$

$$\frac{\partial\Omega_z}{\partial z}=0 \qquad on\ a\ free\ boundary,$$

Linear Stability Analysis

The mathematical treatment of a problem in stability generally proceeds along the following lines:

We start from an initial flow which represents a stationary state of the system. By supposing that the various physical variables describing the flow suffer small (infinitesimal) increments, we first obtain the equations governing these increments. In obtaining these equations from the relevant equations of motion, we neglect all, products and powers (higher than the first) of the increments and retain only terms which are linear in them. The theory derived on the basis of such linearized equations is called the linear stability theory in contrast to non-linear theories which attempt to allow for the finite amplitudes of the perturbations. Stability means stability with respect to all possible (infinitesimal) disturbances. Accordingly, for an investigation on stability to be complete, it is necessary that the reaction of the system to all possible disturbances be examined.

In practice, this is accomplished by expressing an arbitrary disturbance as a superposition of certain basic possible modes and examining the stability of the system with respect to each of these modes.

In accordance with the above described procedure, we assume V and q to be infinitesimal, linearize equations (*X*) and (*Y*), with respect to these variables, then apply the operator z curl curl to (*X*). The system then reduces to two equations for v_z and q. On eliminating q, we fix a horizontal wavevector $\mathbf{k}=\{k_x, k_y, 0\}$, and seek v_z in the form of normal modes:

$$v_z \propto e^{lt}\, w(x)\, f(z)$$

$$l : \textit{the growth rate},$$

$$x = \{x, y, 0)$$

$$\textit{and } w(x) \textit{ is some spatially periodic solution of the Helmholtz equation } \Delta w + k^2 w = 0,$$

$$\textit{i.e., a linear combination}$$

$$w(x) = \sum_{\substack{j=-N \\ (j\neq 0)}}^{N} c_j\, e^{ik_j x}$$

Solving the characteristic equation for stress-free boundaries, we can easily obtain the expression for the eigenvalues l_n corresponding to the eigenfunctions $f_n \sin npz\,(n = 1,2,....)$:

$$l_n = -\frac{P+1}{2}(n^2 p^2 + k^2) \pm \sqrt{(\frac{P-1}{2})^2 (n^2 p^2 + k^2)^2 + \frac{RPk^2}{n^2 p^2 + k^2}}$$

One of these eigen values is always negative, while other is positive if

$$\mathrm{R} > R_n(k) \equiv \frac{(n^2 p^2 + k^2)^3}{k^2}$$

and negative if $R < R_n(k)$.

Each function $R_n(k)$ has a minimum. The line $R=R_1(k)$ in the plane (k, R) delimits the region where all infinitesimal perturbations decay and the region where the lowest perturbation mode n=1 grows.

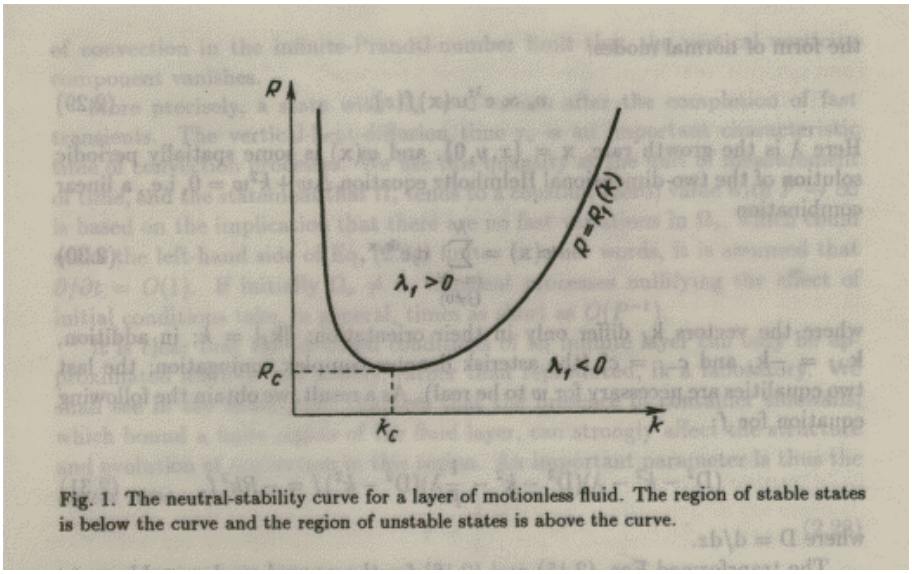

Fig. 1. The neutral-stability curve for a layer of motionless fluid. The region of stable states is below the curve and the region of unstable states is above the curve.

Obviously, if

$R < R_c \equiv \min R_1 (k) = R_1 (k_c)$,

the motionless state of the fluid in the layer is stable with respect to infinitesimal perturbations. The quantities R_c and k_c are termed, respectively, the *critical Rayleigh number* and the *critical wave number*. The critical (neutral) regime ($R=R_c$) corresponds to the onset of steady-state motion with an infinitesimal amplitude and with a unique wave number $k=k_c$. If $R > R_c$ (supercritical regime), the layer is convectively unstable, and those perturbations can grow which have wavenumbers lying between the two roots of the equation $R=R_1(k)$.

For two stress-free boundaries

$$R_c = 657.511, \quad k_c = 2.221$$

For two rigid boundaries

$$R_c = 1707.762, \quad k_c = 3.117$$

and for one rigid and one stress-free boundary

$$R_c = 1100.657 \quad k_c = 2.682$$

Results and Analysis

The classical R-B problem is for an infinite aspect ratio (A.R., defined as the lateral extent to the height) container. But most of the experimental and numerical work have been done for either small (A.R.< 5), or intermediate (5<= A.R.<=20) rectangular boxes. This is due to the following facts:

1) Experiments with the large A.R. boxes are difficult and costly to set up and maintain and computational work would require more processing time due to the choice of a larger grid size.
2) When the Rayleigh # is increased beyond a certain critical value, R-B convection becomes oscillatory. Experimentally (Behringer, 1985 [2]), it was shown that when the Rayleigh # is increased further, flow becomes turbulent soon after in large A.R. enclosures. It is only in small A.R. boxes that R-B convection evolves according a distinct set of bifurcations, ultimately leading to turbulence.
3) For large systems (A.R. >20), the initial time dependence is typically a slow motion of the roll pattern on the time scale of the horizontal-diffusion time. This slow motion makes it difficult to distinguish clearly other changes and instabilities in the pattern.
4) In low A.R. boxes, the dynamic behavior is simpler due to the restricting and pervasive influence of side walls but no less rich due to the highly degenerate and nonunique behavior of the system.

Due to this last point, as mentioned above, the intermediate A.R. boxes have been a preferred choice among the researchers. In their opinion, for smaller boxes, changes in the flow pattern are severely restricted by the boundaries, and the flow becomes time dependent in a manner which is similar to that observed in a dynamical system of low dimensionality (Gollub and Benson 1980 [3]; Dubois and Berge 1980 [4]). It seems unlikely that the dynamics in these systems is closely related to the dynamics in larger fluid systems.

Nonetheless, the presently available results for both small and intermediate sized boxes provide enough insights into the standard problem and in some cases adequately represent the physical situation, where the boundaries are actually finite. In this section, we will report results and analysis for both sizes of boxes.

Pattern formation:

Let us first consider the evolution of classical R-B systems as the nondimensional temperature difference (Rayleigh #) across the fluid layer is increased. Convection begins at some threshold Rayleigh # (Ra_c); below this value there is no flow, and the heat is transmitted by conduction through the fluid. With the presence of horizontal boundaries, with no specific initial conditions imposed, and with no variation of the viscosity with temperature, the first spatial pattern above R_c is found to be a stationary system of parallel rolls. Then, apart from normally present irregularities, or pattern defects, the velocity field of roll convection is nearly two dimensional.

We have seen that at the onset of instability the disturbances which will be manifested will be characterized by a particular wave number. Nevertheless, the pattern which the convection cells will exhibit is completely unspecified. This arises from the fact that a given wave vector can be resolved into two orthogonal components in infinitely many ways; and moreover, the waves corresponding to different resolutions can be superposed with arbitrary amplitudes and phases. If there are no points or directions in the horizontal plane which are preferred, the entire layer in the marginal state must be tessellated into regular polygons with the cell walls being surface of symmetry. Such complete symmetry require that the polygons be either equilateral triangles, squares, or regular hexagons.

If n is the number of the sides of the regular polygon, then the angle at a vertex (= $p\,(1-2/n)$*) must divide* $2p$ *an integral number of times. Hence we must have 1-2 / n = 2 / m, where m is an integer; this relation can be satisfied only for n=3, 4, and 6, when m=6, 4, and 3, respectively.*

Thus, the observed roll pattern is just one of the possibilities. Among the cells observed experimentally under varying conditions, the following two types of planform are mostly found:

1. *Two-dimensional rolls:* A particularly simple pattern occurs when all the quantities depend on only one of the horizontal direction, say x. In this case, the cells are infinitely elongated and it is more appropriate to call them rolls. They have a prototype given by the function

$$w(\mathbf{x}) = \cos \mathbf{kx}$$

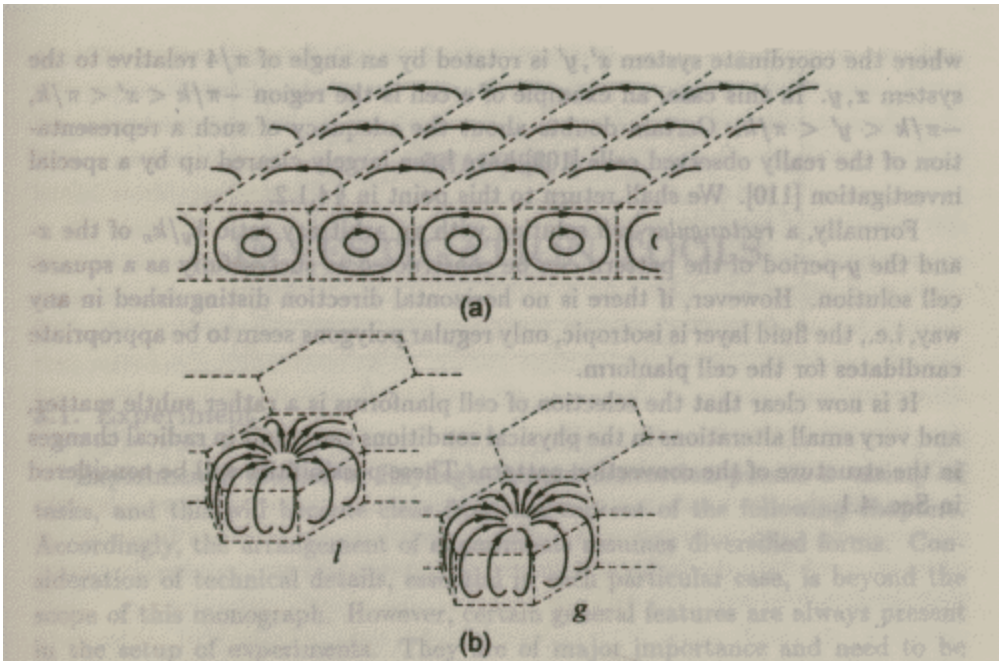

Fig. 3. Schematic diagram of convection cells. (a) Two-dimensional rolls. (b) Hexagonal *l*- and *g*-cells.

2. *Hexagonal cells*: This system is a superposition of three roll sets with wavevectors having the same modulus k and directed at an angle of $2p/3$ to one another. A hexagonal cell is called an *l*- or a *g- cell* depending on the sign of the velocity (i.e., on whether the fluid ascends or descends in the central part of the cell). *g-cells* are usually observed in the gases (hence named *g*-) and *l-cells* are seen often in the liquid (hence named *l*-). Graham [5] argued that the direction of circulation should depend on the sign of the derivative $\partial n/\partial T$ which is as a rule negative for liquids and positive for gases. The ascending fluid in a convection cell is always warmer than the descending fluid. Therefore, the central part of an *l-cell* is less viscous for liquids, and the central part of a *g-cell,* for gases. We see that the realized direction of circulation is that at which viscous stresses are weaker near the axis of the cell.

It is clear by now, that the preference can not be given to any convection-cell planform because of the degeneracy of the solutions with respect to planforms. Thus, there arises the issue of

determining the planforms that would be really observed under the corresponding conditions. The stability analysis of various planforms can be applied as the first step in resolving this issue.

As shown in a photograph above, Bénard observed flow patterns consisting of polygonal, mainly hexagonal cells with upflow at the centre of each cell and down flow at the periphery. The most regular patterns of this type have honeycomb symmetry. We seek to remove the longstanding confusion about the appropriate reasons behind this structure. These cells were mainly due the thermocapillary action accompanied by top free surface. In contrast, thermogravitational convection mainly produces roll patterns. Thus, as it stands, under the standard conditions, quasi-two-dimensional rolls represent the basic form of steady-state convection as first critical Rayleigh # is achieved.

Patterns of Quasi-Two-dimensional Rolls

As we saw, if there are no complicating factors, a roll pattern is the basic form of steady-state convection. Even if a roll pattern is very regular and free of defects, the rolls nonetheless are usually not completely straight and the flow in them is not completely two dimensional. This happens, at the very least, because of the fact that in reality the flow always involves only a a portion of an infinite layer, bounded by sidewalls which can have a considerable effect on the flow structure.

The presence of sidewalls removes the degeneracy of the eigenfunctions: in a rectangular box with rigid horizontal and vertical boundaries the critical Rayleigh # is smaller for those rolls which are parallel to the shorter side of the container. For a square container, the mutually perpendicular rolls can also rise in the neighborhood of the instability threshold.

Many experimental data have shown that the indicated roll orientation is a particular case of a more general tendency: rolls tend to approach a wall at a right angle. This tendency is noticeable where it results in a considerable bending of rolls and therefore, in forming textures. This is shown below, where the rolls in the bulk of the container make large angles with the normals to the walls. Another example, typical of round containers, is shown in the other figure (this pattern, which resembles the logo of the Pan American Airlines, is sometimes called the "Pan Am texture").

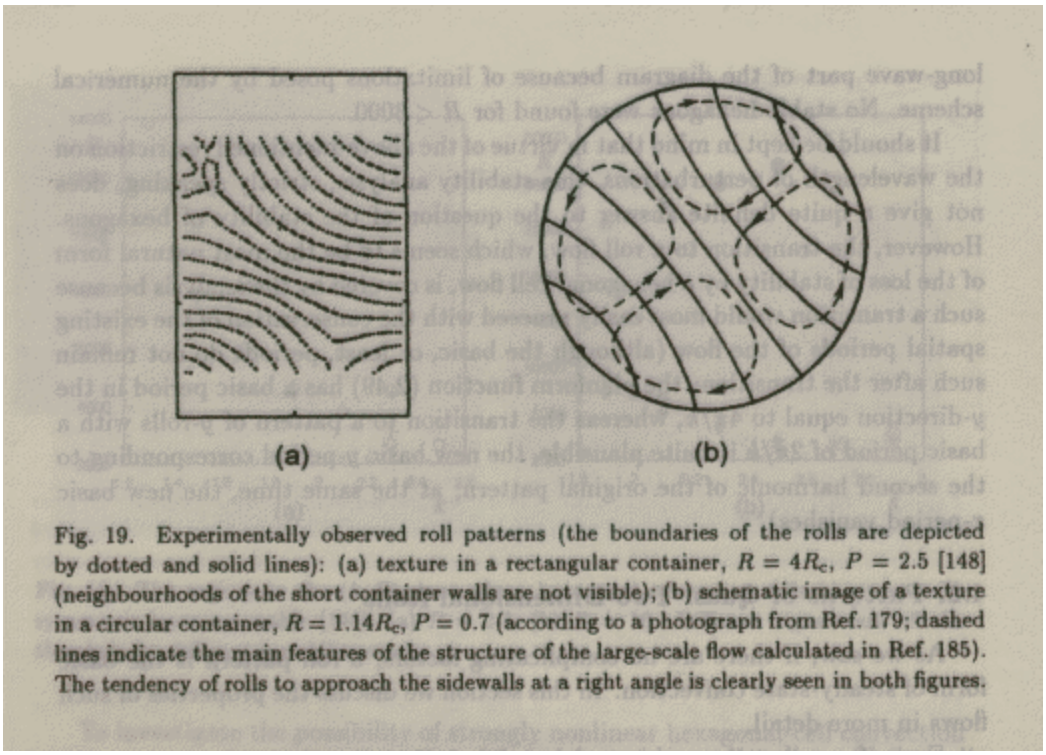

Fig. 19. Experimentally observed roll patterns (the boundaries of the rolls are depicted by dotted and solid lines): (a) texture in a rectangular container, $R = 4R_c$, $P = 2.5$ [148] (neighbourhoods of the short container walls are not visible); (b) schematic image of a texture in a circular container, $R = 1.14R_c$, $P = 0.7$ (according to a photograph from Ref. 179; dashed lines indicate the main features of the structure of the large-scale flow calculated in Ref. 185). The tendency of rolls to approach the sidewalls at a right angle is clearly seen in both figures.

Convection Textures: Roll pattern defects

Relatively ordered roll patterns in which the directions of rolls varies in space slowly, even if over wide limits are termed *textures*. Also *complex textures* are commonly observed in which several ordered fragments, or textures in the indicated sense can be isolated. The presence of defects imparts to the system additional "degrees of freedoms". Readjustment of the roll wavenumber in the process of seeking the optimum value occurs most easily in the presence of pattern defects. Typical defects of roll patterns are described below:

1) Dislocations

A dislocation is a defect arising at a point where an "extra" pair of rolls, wedged into a regular roll pattern, terminates (the rolls being somewhat bent near the dislocation). In most cases dislocations move in a direction parallel to the rolls (*climb*), though sometimes movement in a perpendicular direction (*glide*) are also seen. Fig (a)

2) Disclinations:

Disclinations are defects corresponding to singularities in the filed of directors (vectors without arrows) obtained from the local wavevectors of the pattern. A dislocation can be regarded as the superposition of two disclinations. Fig (b)

3) Grain boundaries

A defect of a very characteristic type is a *grain boundary*, i.e., a line along which two ordered patches (or textures) of rolls of different orientation come together, comprising a more complex pattern, as shown in fig. (c).

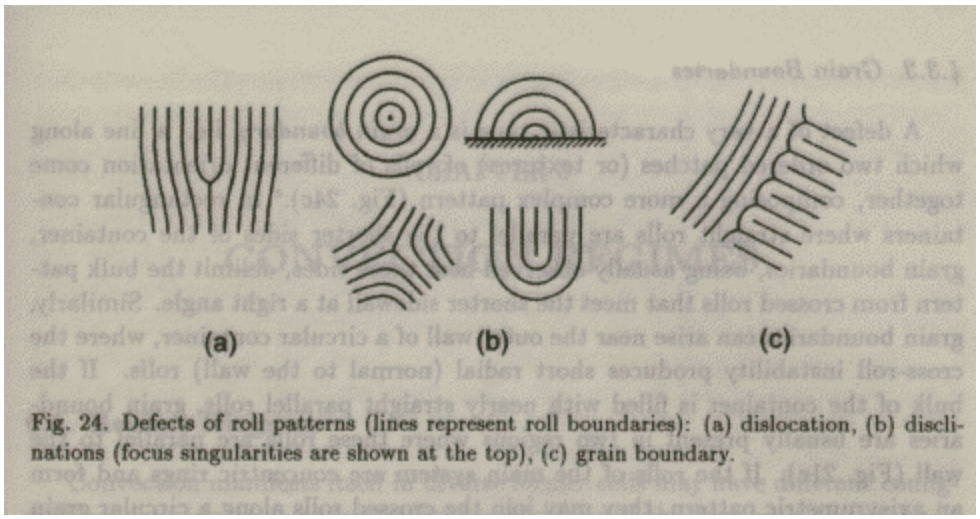

Fig. 24. Defects of roll patterns (lines represent roll boundaries): (a) dislocation, (b) disclinations (focus singularities are shown at the top), (c) grain boundary.

Defects of roll pattern

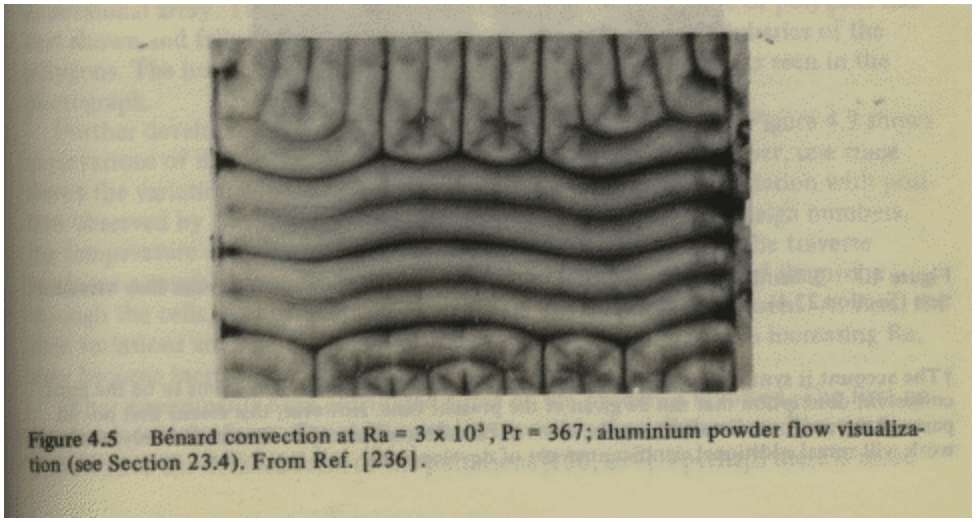

Figure 4.5 Bénard convection at Ra = 3 x 10^3, Pr = 367; aluminium powder flow visualization (see Section 23.4). From Ref. [236].

Presence of grain boundaries

Tertiary Flows

The flows arising due to the instability of a roll flow, are termed tertiary flows, implying that the original roll flow is regarded as secondary flow.

Roll convection is observed only in a certain range of Rayleigh #, which depends on the Prandtl #. Beyond the upper limit of this range rolls become unstable and tertiary flows develop, making the velocity field three dimensional. Here we describe some instability types that produce flow patterns of remarkable appearance, greatly affected by tertiary flows.

The *cross-roll instability* manifests itself in the nucleation of a new system of rolls perpendicular to the original rolls. In essence, this is an instability of the boundary layers produced by the fluid circulation in the original rolls. At moderately high Rayleigh #, the crossed rolls finally replace the original rolls. At higher Rayleigh #, $R > 10R_c$, the cross-roll instability results in the development of a so-called *bimodal* flow. This is a superposition of the two roll sets.

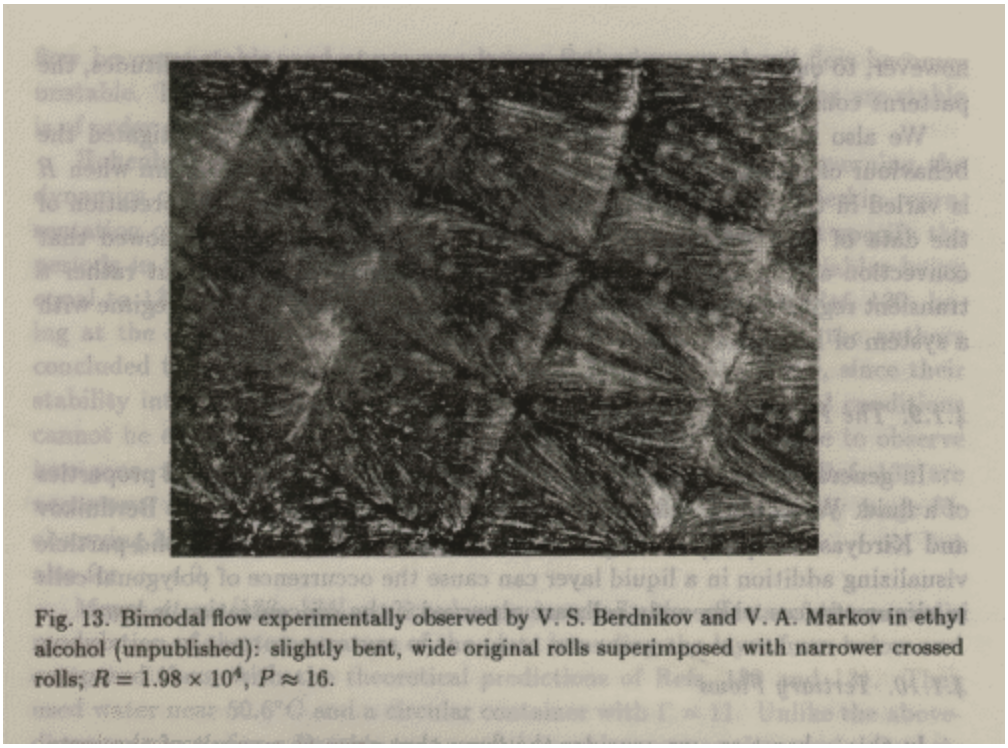

Fig. 13. Bimodal flow experimentally observed by V. S. Berdnikov and V. A. Markov in ethyl alcohol (unpublished): slightly bent, wide original rolls superimposed with narrower crossed rolls; $R = 1.98 \times 10^4$, $P \approx 16$.

bimodal flow

At R values as large as $R \approx 10^5$ the original rolls no longer appear as the basic flow and bimodal convection assumes the form of a pattern of *rectangular cells*.

The cross-roll instability has also a long-wave branch, with the tertiary-flow wavenumber less than k_c, which is known as the *Knot instability* and observed at moderate Pr #. At sufficiently

large Rayleigh # it results in the formation of highly concentrated rising and falling plumes (see figure below).

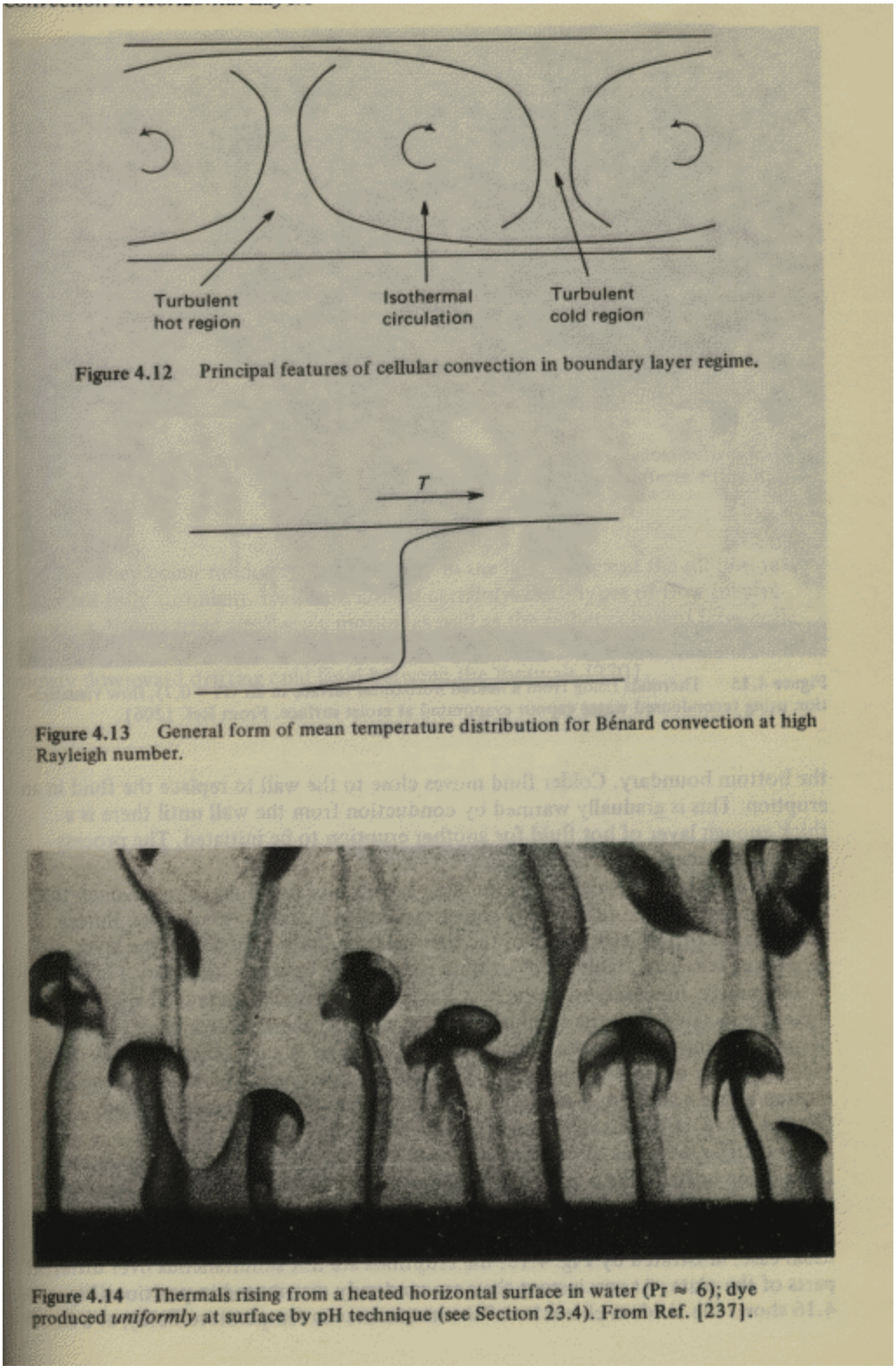

Figure 4.12 Principal features of cellular convection in boundary layer regime.

Figure 4.13 General form of mean temperature distribution for Bénard convection at high Rayleigh number.

Figure 4.14 Thermals rising from a heated horizontal surface in water (Pr ≈ 6); dye produced *uniformly* at surface by pH technique (see Section 23.4). From Ref. [237].

Thermal plumes

Fully developed knot convection acquires the form of *spoke-pattern convection* in which the original roll structure is replaced by a polygonal pattern. Sheets of hot and cold fluid, erupting from the thermal boundary layers at the top and the bottom surface, are stretched radially with respect to the plumes and appear like spokes.

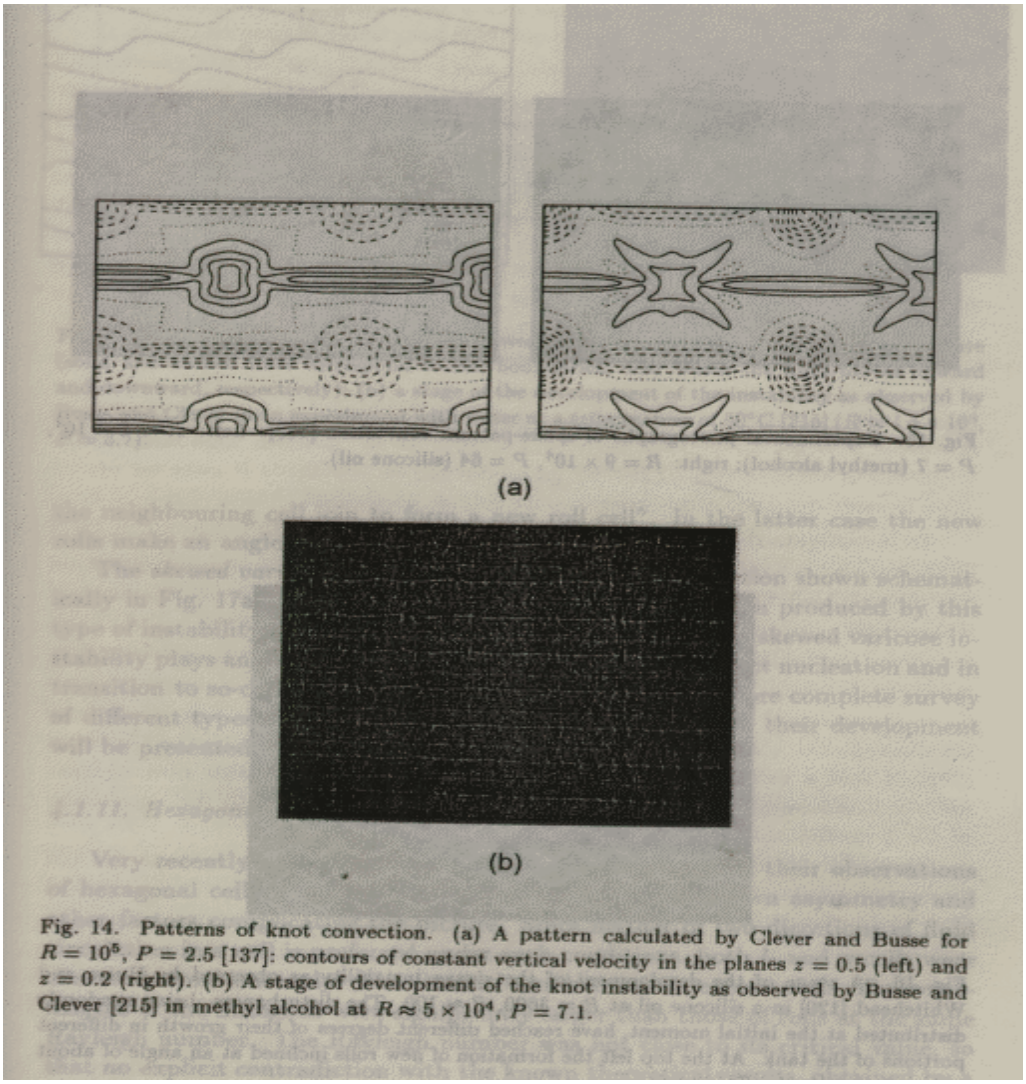

Fig. 14. Patterns of knot convection. (a) A pattern calculated by Clever and Busse for $R = 10^5$, $P = 2.5$ [137]: contours of constant vertical velocity in the planes $z = 0.5$ (left) and $z = 0.2$ (right). (b) A stage of development of the knot instability as observed by Busse and Clever [215] in methyl alcohol at $R \approx 5 \times 10^4$, $P = 7.1$.

knot instability

The *zig-zag instability* bends the original rolls to form a pattern of wavy or undulating rolls. The *skewed-varicose instability* results in a roll deformation as shown schematically in the fig. below Skewed Varicose instability plays an important role in the process of pattern-defect nucleation and in transition to so-called phase turbulence.

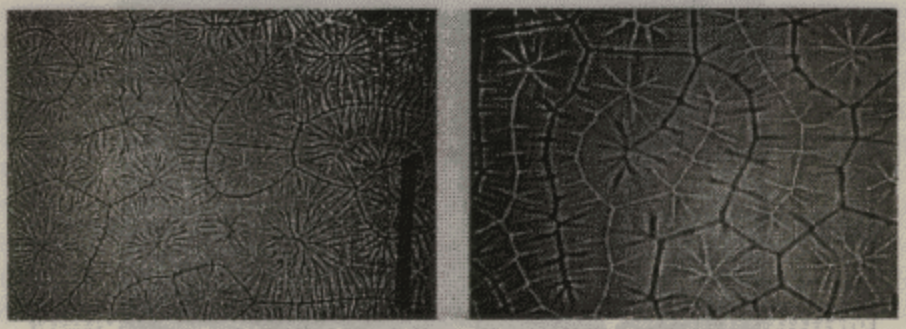

Fig. 15. Experimental photographs of spoke-pattern convection [138]. Left: $R \approx 5 \times 10^4$, $P = 7$ (methyl alcohol); right: $R = 9 \times 10^4$, $P = 64$ (silicone oil).

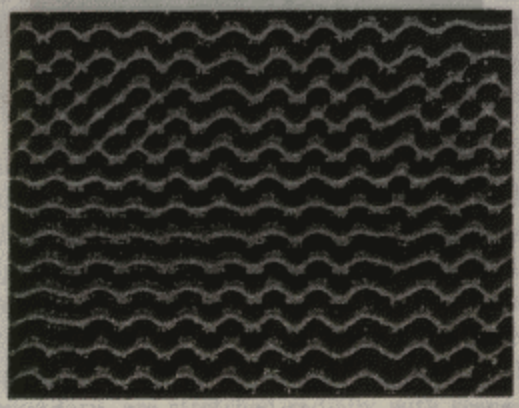

Fig. 16. A stage of the development of the zigzag instability as observed by Busse and Whitehead [120] in a silicone oil at $R = 3600$, $P \approx 100$. The disturbances, being randomly distributed at the initial moment, have reached different degrees of their growth in different portions of the tank. At the top left the formation of new rolls inclined at an angle of about 45° to the original rolls is seen.

Spoke like pattern development and zig-zag instability

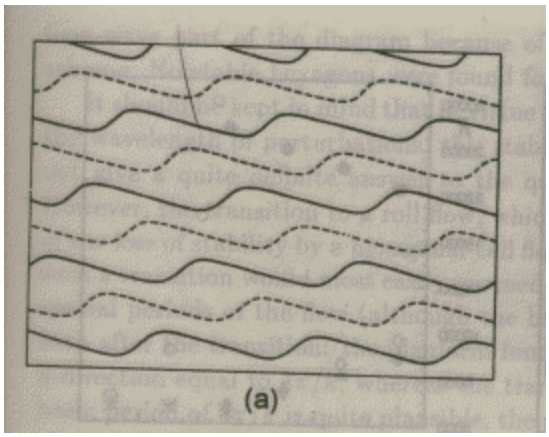

The skewed varicose instability

Transitions

Temporal transition

As described above, transitions in small boxes are most rich in the features. Therefore, let us take a case study ([6]) for a box of A.R.3.5. Its is seen that in a small A.R. box, flow undergoes a sequence of bifurcation from steady state to oscillatory convection to chaos. With an initial configuration consisting of two symmetric rolls, as the Rayleigh # is increased, steady state is lost at a certain Rayleigh # and oscillatory regime begins.

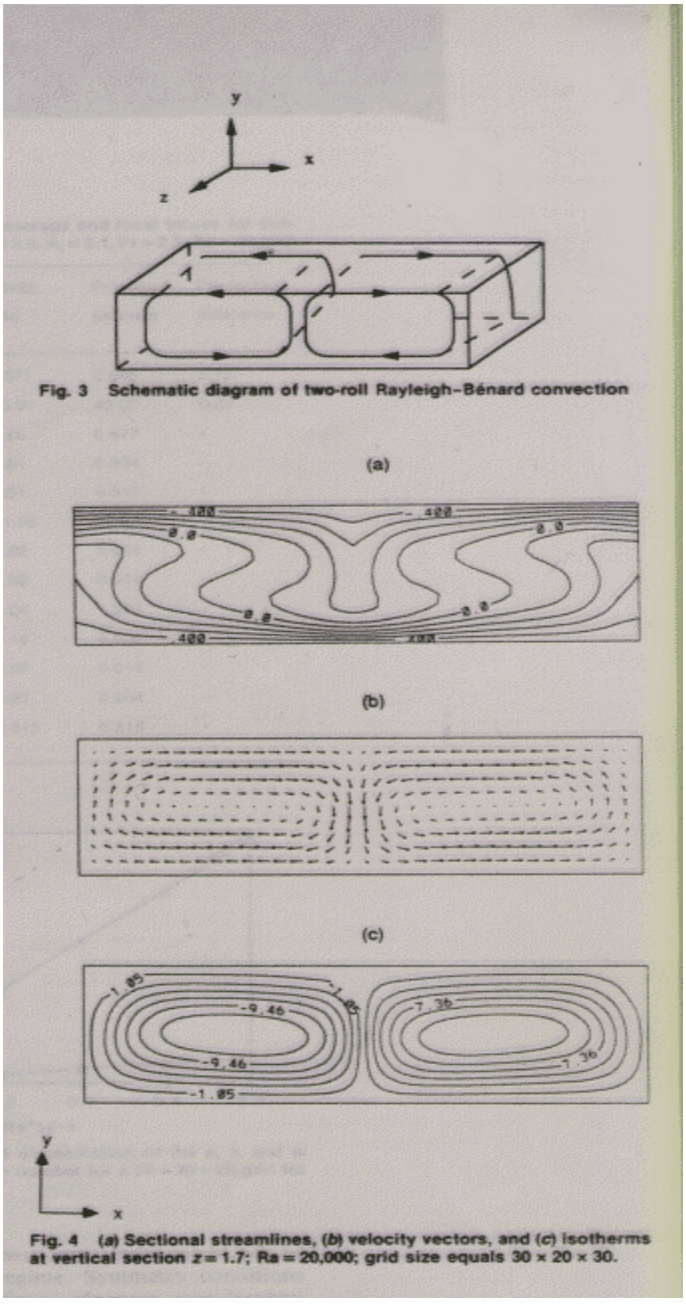

Fig. 3 Schematic diagram of two-roll Rayleigh–Bénard convection

Fig. 4 (*a*) Sectional streamlines, (*b*) velocity vectors, and (*c*) isotherms at vertical section $z = 1.7$; Ra = 20,000; grid size equals 30 × 20 × 30.

This critical Rayleigh # is determined by extrapolation. The square of the amplitude of oscillation of three velocity components as a function of Rayleigh number shows a linear variation (see fig. below).This functional dependence is consistent with stability theory. Extrapolation to zero velocity amplitude of oscillation shows that the critical Ra # is around 30,000.

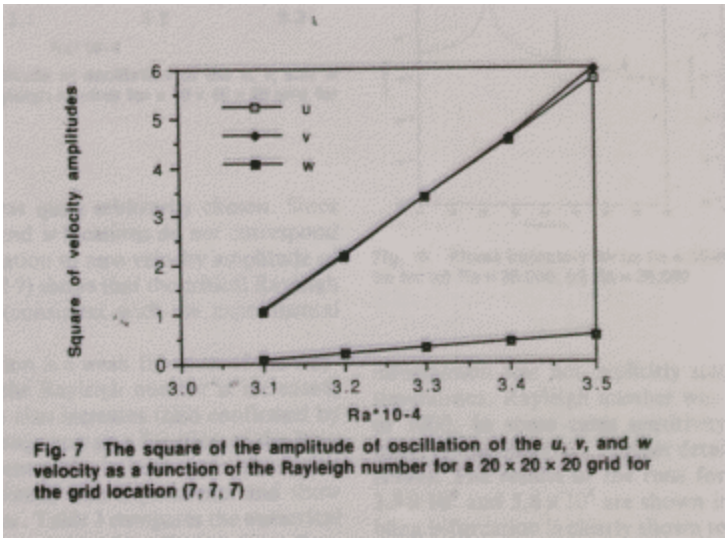

Fig. 7 The square of the amplitude of oscillation of the *u*, *v*, and *w* velocity as a function of the Rayleigh number for a 20 × 20 × 20 grid for the grid location (7, 7, 7)

The square of the amplitude of oscillation of the u, v, and w

With further increase in Rayleigh number the Period-doubling bifurcation is encountered at Rayleigh # 36000, as is clear from the following power spectra

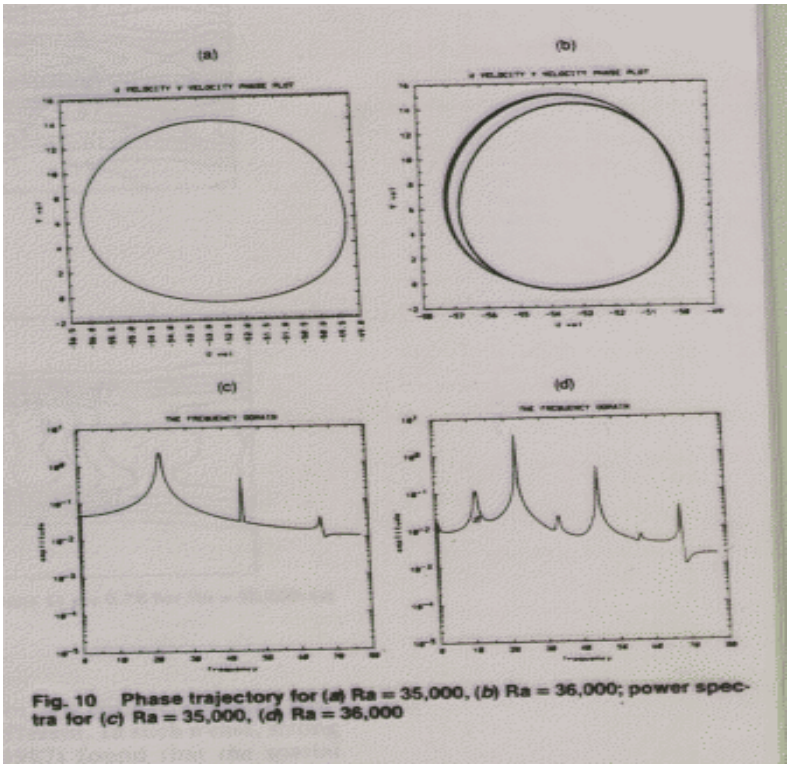

Fig. 10 Phase trajectory for (*a*) Ra = 35,000, (*b*) Ra = 36,000; power spectra for (*c*) Ra = 35,000, (*d*) Ra = 36,000

Phase trajectory and power spectra

Th oscillating temperature filed (at Ra # =35,000) as a function of time was looked into by taking snapshots. The figure below indicates that the oscillations consist of standing waves propagating along the roll axis. As a result of reflection off the walls, a standing wave pattern is created instead of travelling wave in a horizontally unbounded domain.

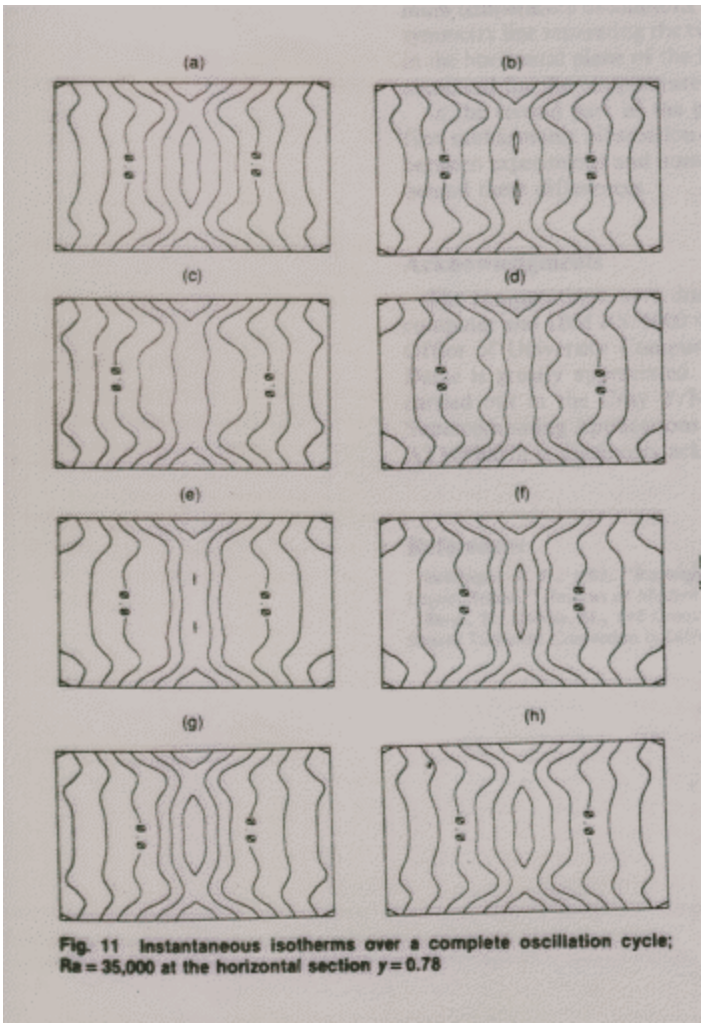

Fig. 11 Instantaneous isotherms over a complete oscillation cycle; Ra = 35,000 at the horizontal section $y = 0.78$

Standing wave-pattern

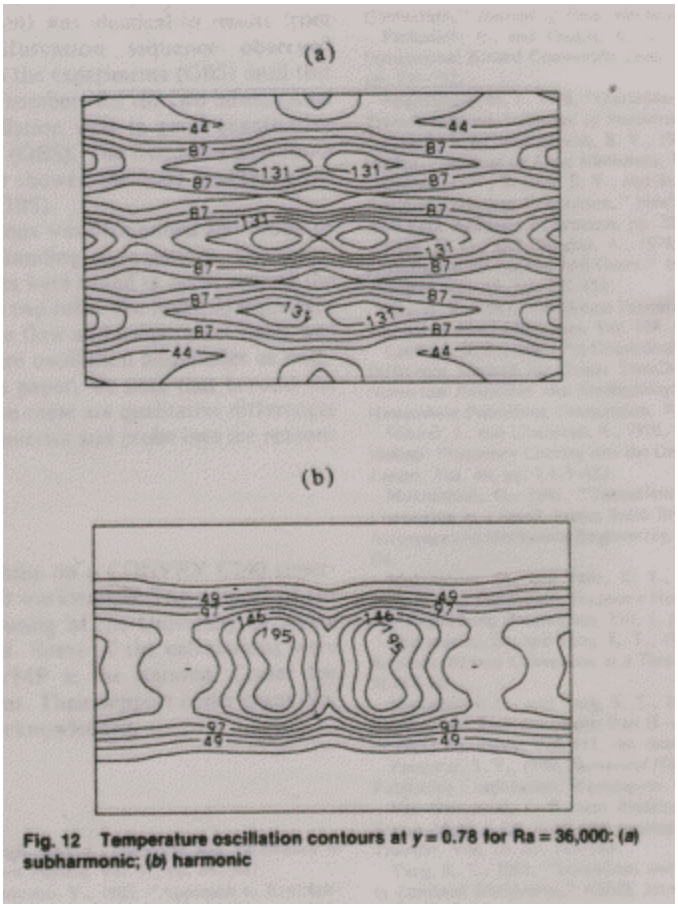

Fig. 12 Temperature oscillation contours at $y = 0.78$ for $Ra = 36{,}000$: (*a*) subharmonic; (*b*) harmonic

Four fold symmetry, as seen in Temperature oscillation contours

Contour maps of the amplitude of the subharmonic and fundamental frequency of temperature oscillations are shown above. The Rayleigh number is 36,000, just above the subharmonic bifurcation. the contours correspond to the same horizontal location as in the previous figure. A fourfold symmetry is seen in the oscillation amplitude contours for both the fundamental and subharmonic. This fourfold symmetry is a crucial feature. With further increase in Rayleigh #, quasi-periodicity (with a low-frequency component) was seen followed by chaos, which was observed at 39000-410000. The route to chaos is the Ruelle-Takens-newhouse scenario.(P->QP->Chaos). Another route to chaos is observed when the bifurcation sequence consists of an infinite sequence of subharmonic bifurcations until the onset of chaos. This is known as Feigenbaum sequence. Work presented by [6] observed that this sequence got terminated after one periodic doubling bifurcation (P1->P2->QP->Chaos), in another experimental work [7] observed one more subharmonic bifurcation before the quasi-periodicity sets in followed by chaos.

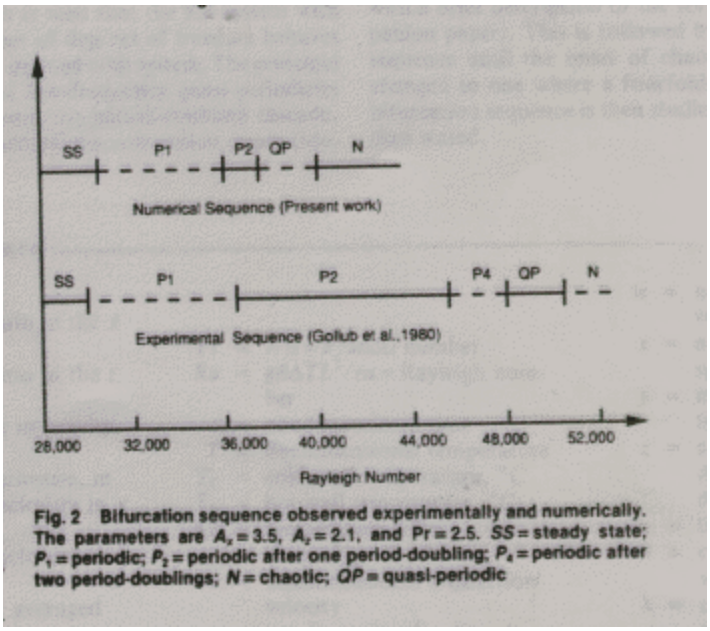

Fig. 2 Bifurcation sequence observed experimentally and numerically. The parameters are $A_x = 3.5$, $A_z = 2.1$, and $Pr = 2.5$. *SS* = steady state; P_1 = periodic; P_2 = periodic after one period-doubling; P_4 = periodic after two period-doublings; *N* = chaotic; *QP* = quasi-periodic

Bifurcation sequence for two different work

Bifurcation sequences are strong function of thermal history and the step change in Rayleigh number, and therefore, the differences are observed. If the fourfold symmetry is maintained (which actually gets lost at second period-doubling bifurcation, $Rayleigh_{c=}46000$), further few such bifurcations are seen, although it becomes increasingly difficult to pinpoint subsequent bifurcations since bifurcation points get closer and closer.

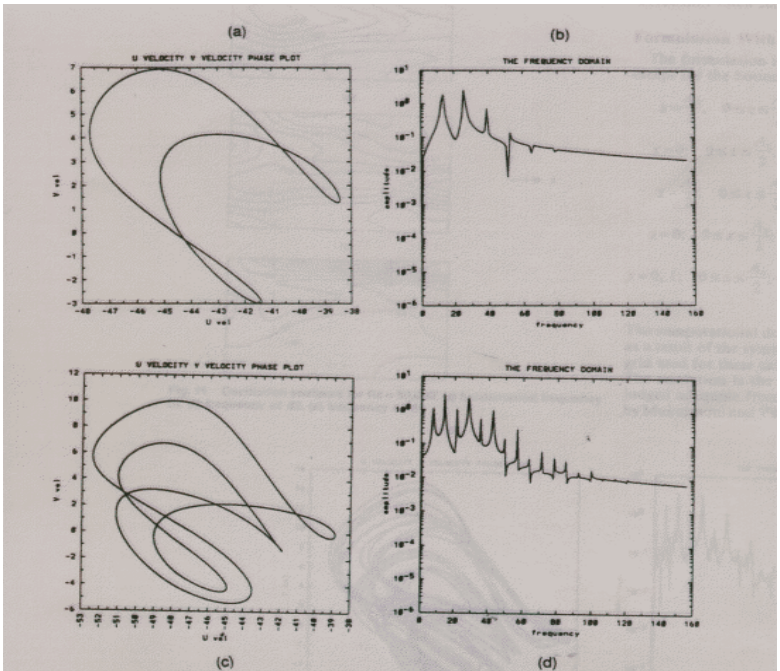

Fig. 10 (*a*) Phase trajectory, (*b*) spectral amplitudes for Ra = 47,000; (*c*) phase trajectory, (*d*) spectral amplitudes for Ra = 48,000

Another bifurcation at Rayleigh # = 48,000

Thus, it was found that the Feigenbaum scenario could be observed, and no low-frequency quasi-periodicity was encountered. This makes it quite clear that is the asymmetry between the rolls that terminates the Feigenbaum sequence and the introduced quasi-periodicity. The bifurcation sequence for the set of parameters is therefore nonunique. The most common scenario, it seems, is a finite cascade of period-doubling followed by quasi-periodicity (with a low frequency) and subsequent chaos.

Spatial Transition

- Above, we described a case of flow transitions primarily restricted to small enclosures and temporal transitions. Now, let us discuss a case of spatial transitions in small and intermediate boxes.

It has long been known that the R-B problem is degenerate, i.e., for the same set of governing parameters many solutions are possible. This is a consequence of the nonlinearity of the problem. The mechanism on how different solutions to the problem evolve and compete and the process by which a particular flow configuration undergoes changes is broadly known as pattern selection. One well documented phenomenon experimentally observed in small and rectangular boxes is the decrease in the number of rolls with an increase in Rayleigh number. According to linear stability theory, the loss of roll is due to the skewed-varicose instability. [8] reported few such instances. In one work, they showed that for a small box (4:2:1) for a Pr # 0.71, the number of rolls changed from 4 to3. The transition sequence shows the typical thinning and thickening of the distorted rolls in time sequence. (see figure below)

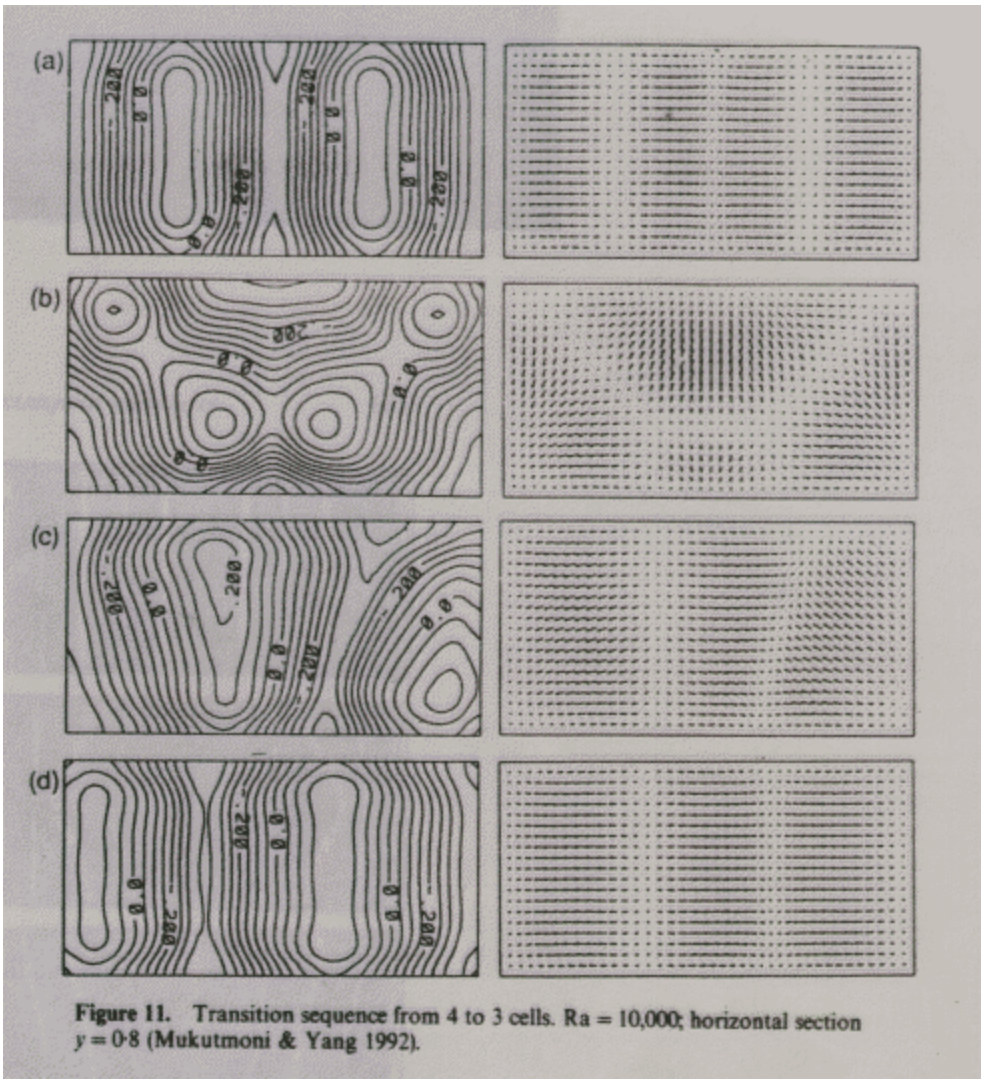

Figure 11. Transition sequence from 4 to 3 cells. Ra = 10,000; horizontal section $y = 0{\cdot}8$ (Mukutmoni & Yang 1992).

Transition sequence from 4 to 3 cells. Rayleigh =10,000

- Now, consider the following stability diagram for a fluid of Prandtl number 3.5 and 15, assuming infinite lateral boundary conditions:

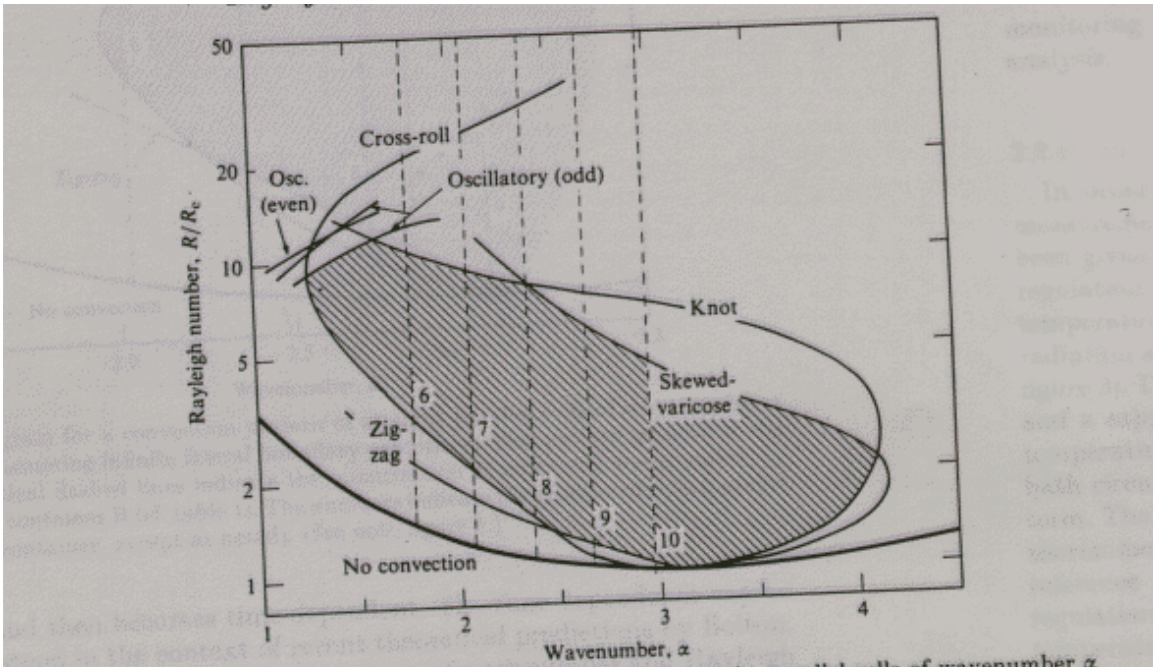

FIGURE 1. Stability diagram for a convection pattern of straight parallel rolls of wavenumber α for Prandtl number 3.5 assuming infinite lateral boundary conditions. This pattern is stable in the shaded region. The vertical dashed lines indicate the quantization of mean roll wavenumber by the finite aspect ratio of container A (cf. table 1). The numbers indicate the number of rolls parallel to the short side of the container. *Note*. The calculated stability boundaries presented in this paper are interpolated and extrapolated from the calculations of Busse, Bolton, and Clever (Busse & Clever 1979; Busse 1978; Bolton, Busse & Clever 1983; and private communications). Although the curves presented should be qualitatively correct, uncertainties of 10–20 % are possible in some cases.

Stability diagram for Prandtl number=3.5

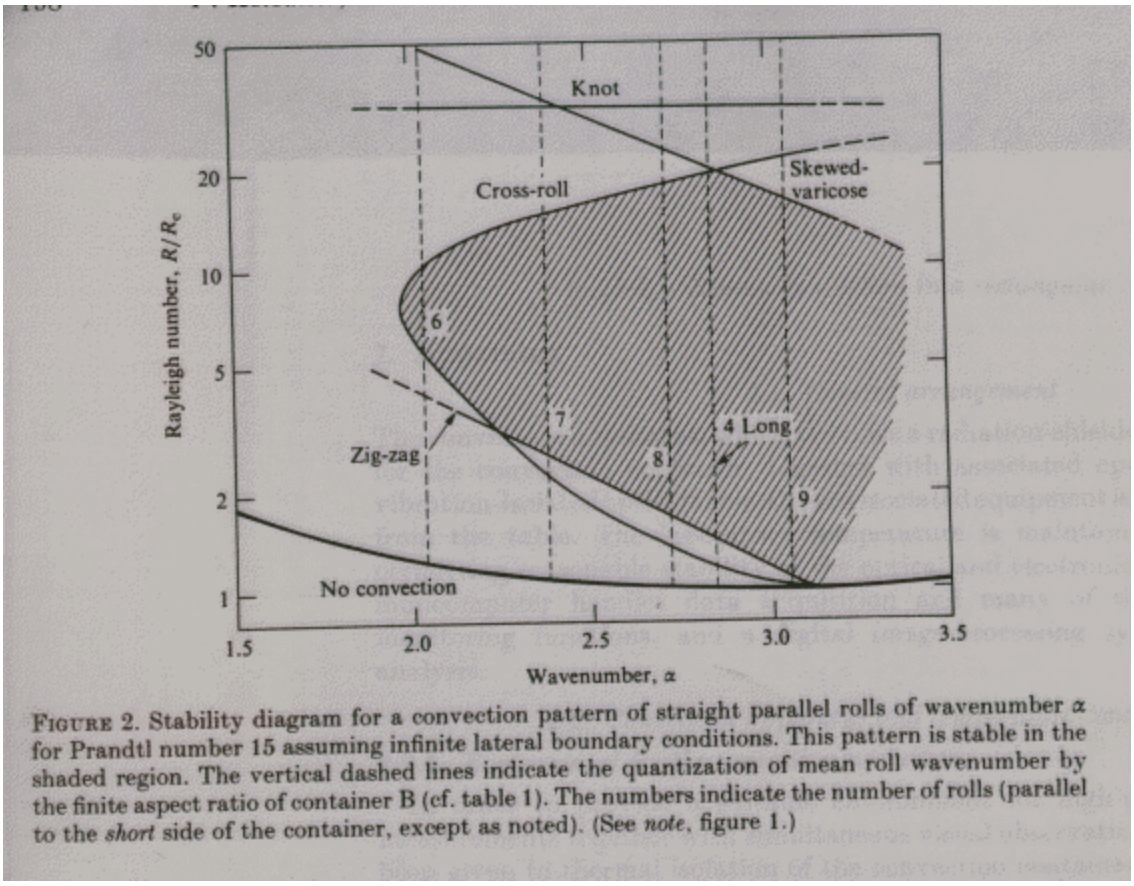

FIGURE 2. Stability diagram for a convection pattern of straight parallel rolls of wavenumber α for Prandtl number 15 assuming infinite lateral boundary conditions. This pattern is stable in the shaded region. The vertical dashed lines indicate the quantization of mean roll wavenumber by the finite aspect ratio of container B (cf. table 1). The numbers indicate the number of rolls (parallel to the *short* side of the container, except as noted). (See *note*, figure 1.)

Stability diagram for Prandtl number=15

This diagram shows the regions of stability for the given Pr number fluid. The extent of the shown contours is a strong function of Pr number, as is clear from the following figure.

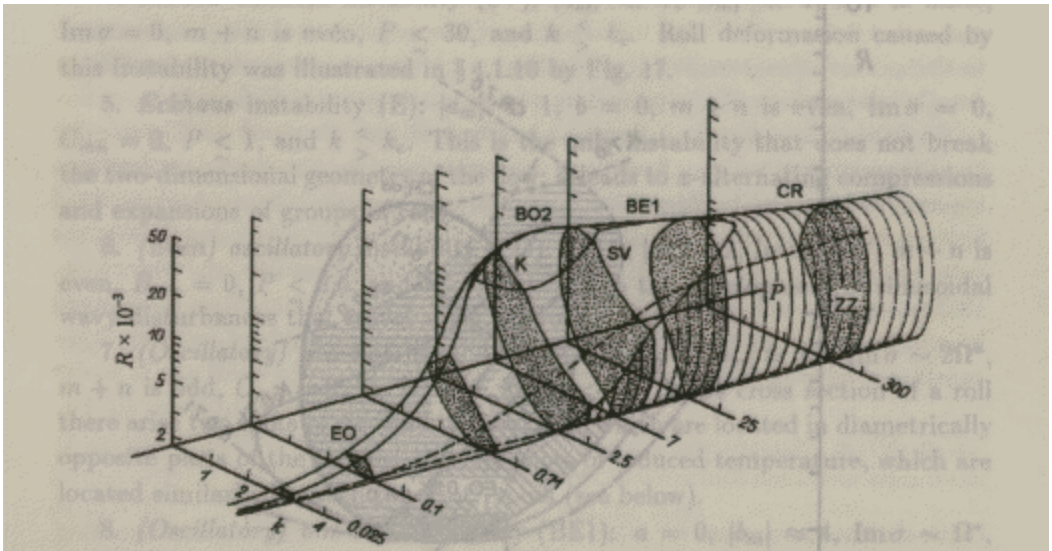

Fig. 34. Region of stability of spatially periodic roll patterns in the (k, P, R)-space ("Busse windsock"); adapted from Ref. 222. By convention, the stability diagram calculated for $P = \infty$ is placed in the plane $P = 300$. No-slip boundary conditions are assumed for the horizontal surfaces of the layer. The portions of the surface bounding the stability region which correspond to particular types of instability are labelled by the letters denoting these types.

Region of stability of periodic roll patterns in the (k, P, R) space

Below the heavy solid line in the first figure, there is no fluid motion. In the shaded regions in Rayleigh # and wavenumber space, convection in a pattern of straight parallel rolls is stable. Beyond these regions, parallel-roll convection is unstable to the various instabilities indicated by the lighter solid lines. In contrast to the case of infinite A.R., one important effect of a container of finite A.R. is that it must contain an integral number of rolls. To a first approximation (i.e., assuming constant wavelength), this means that the wavenumber is quantized. The dashed vertical lines identify the mean wavenumbers corresponding to the integral number of rolls. Assuming, that this diagram (Pr=3.5) is applicable to finite boxes, a state with 9 parallel rolls at a $Ra/Ra_c = 7$, is unstable to the skewed varicose instability. Possible stable states of the system at this Rayleigh # include flow patterns with 6, 7, or 8 parallel rolls. As another example of pattern evolution, consider for Pr=3.5, a stable pattern of six rolls at Rayleigh number of $9Ra_c$. As Rayleigh # is further increased, the system of parallel rolls become unstable for all wavenumbers at about 13Rc. With increasing Ra # the rolls become distorted and then becomes time-dependent. For Pr=15, a different sequence of instabilities is encountered as the Rayleigh # is increased above Rc. At a wavenumber corresponding to 9 rolls, the skewed varicose instability is encountered at $R=17R_c$. For fewer rolls, the first boundary encountered above R_c is that of cross-

roll instability. It is this instability which is known to trigger bimodal convection at $R=10R_c$. The resulting fluid flow is a superposition of secondary rolls located in the boundary layer and oriented at right angles.

An illustration for a box of 10 x 5 x 1size is shown below in which 10 to 8 rolls transition is shown for Pr=3.5:

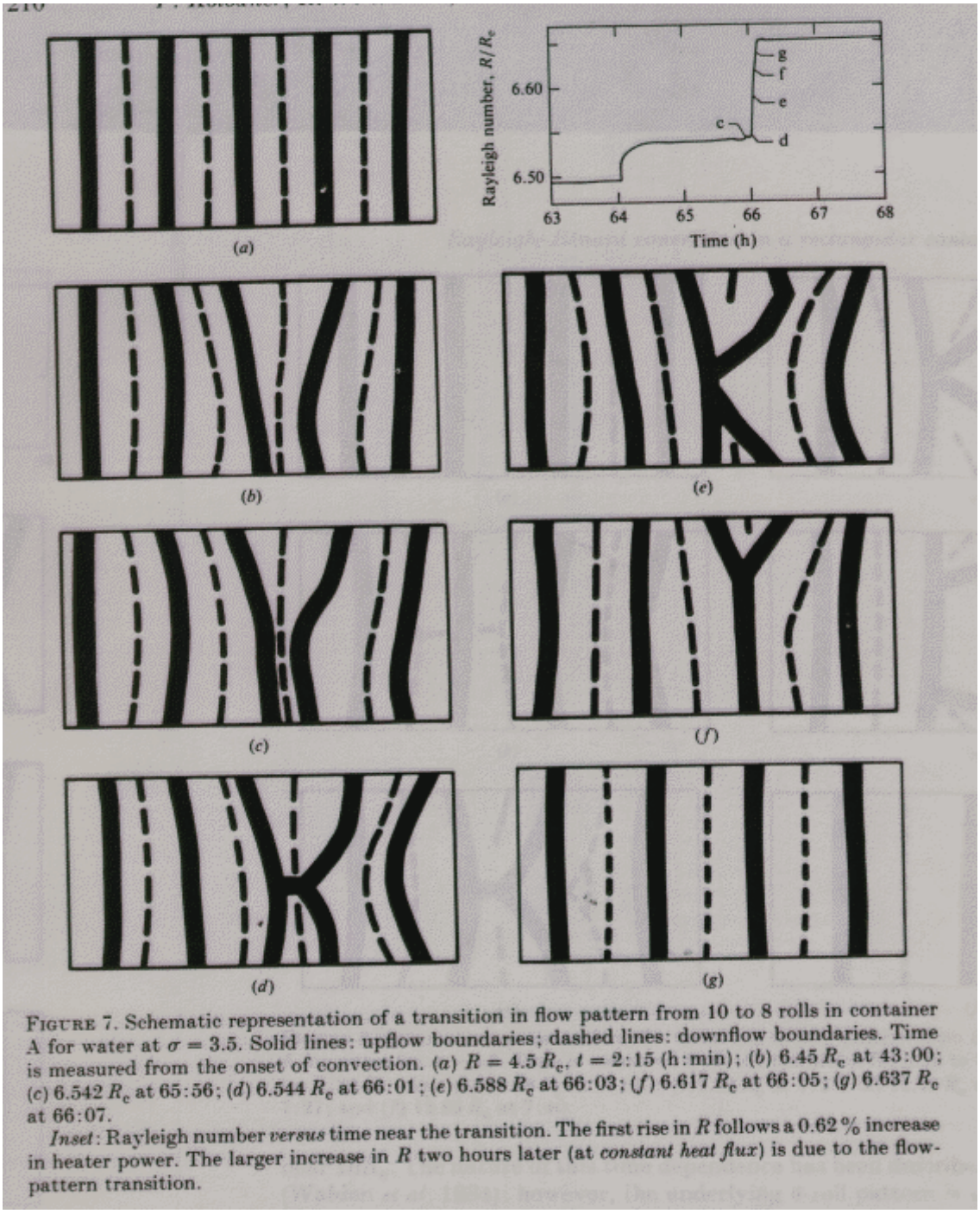

FIGURE 7. Schematic representation of a transition in flow pattern from 10 to 8 rolls in container A for water at $\sigma = 3.5$. Solid lines: upflow boundaries; dashed lines: downflow boundaries. Time is measured from the onset of convection. (*a*) $R = 4.5\,R_c$, $t = 2{:}15$ (h:min); (*b*) $6.45\,R_c$ at 43:00; (*c*) $6.542\,R_c$ at 65:56; (*d*) $6.544\,R_c$ at 66:01; (*e*) $6.588\,R_c$ at 66:03; (*f*) $6.617\,R_c$ at 66:05; (*g*) $6.637\,R_c$ at 66:07.

Inset: Rayleigh number *versus* time near the transition. The first rise in R follows a 0.62 % increase in heater power. The larger increase in R two hours later (at *constant heat flux*) is due to the flow-pattern transition.

Conclusion

This term paper discussed some of the experimental and computational work performed over a period of years on the classic problem Rayleigh-Bénard Convection. The emphasis was on flow transitions, instabilities and bifurcations, and pattern selection. The discussion was restricted to small and intermediate aspect ratio boxes with sidewalls. In the patter formation section, we discussed under what conditions, which planforms are preferred and how do the patterns readjust to a different structure under instability. This was followed by a discussion on temporal and spatial instability. An important conclusion to the considered discussion is that the realizability of a flow is not identical to its stability. The realization of various stable states is not equally probable, so that the class of stable states can in general be much wider than the class of states that are realized under the natural condition.

References

[1] A.C. Newell, T. Passot, and J.Lega, Order parameter equations for patterns, Annual Rev. Fluid Mechanics. 25, 399-453 (1993)

[2] Behringer, R.P., 1985, "Rayleigh-Bénard convection and Turbulence in liquid Helium", Reviews of Modern Physics, Vol 57, pp 657-687

[3] Gollub j.p. and benson S.V. 1980, Many routes to turbulent convection, Journal of Fluid Mechanics, pp 449-470

[4] Dubois M. and Bergi P., 1980, Experimental evidence for the oscillations in a convective biperiodic regime, Phy. Letters 76A, 53-56

[5] A. Graham, Shear pattern in an unstable layer of air, Phil. Trans. Roy. Soc. A232(714), 285-296 (1933)

[6] D. Mukutmoni, K.T. Yang, 1993, Rayleigh-Bénard convection in a small Aspect ratio Enclosure: Part I-Bifurcation to Oscillatory Convection, Journal of Heat Transfer, Vol.115

D. Mukutmoni, K.T. Yang, 1993, Rayleigh-Bénard convection in a small Aspect ratio Enclosure: Part II-Bifurcation to Chaos, Journal of Heat Transfer, Vol.115

[7] Gollub j.p. and benson S.V. 1980, Many routes to turbulent convection, Journal of Fluid Mechanics, pp 449-470

[8] D. Mukutmoni, K.T. Yang, 1994, Flow transitions and pattern selection of the Rayleigh-Bénard problem in rectangular enclosures, Sadhana, Vol. 19, pp 649-670

[9] K.R. Kirchartz and Oertel H. Jr., 1988, Three Dimensional thermal cellular convection in rectangular boxes, J. Fluid Mechanics, Vol. 192, pp 249-286

[10] Jiro Mizushima, 1994, Mechanism of the pattern Formation in Rayleigh-Bénard Convection, Journal of the physical society of Japan, Vol 63, pp 101-110

[11] J. Pallares, F.X. Grau, Francese Giralt, 1999, Flow Transitions in laminar Rayleigh-Bénard convection in a cubical cavity at moderate Rayleigh numbers, Int. J. of Heat and Mass Transfer, Vol. 42, pp 753-769

[12] Arroyo M.P. and Saviron J.M., 1992, Rayleigh-Bénard convection in a small box: spatial features and thermal depedence of the velocity field, J. Fluid Mechanics, Vvol. 235, pp325-348